Persistent-current magnetizations of Nb_3Sn Rutherford cables and extracted strands

IOP Conf. Series: Materials Science and Engineering **279** (2017) 012037 doi:10.1088/1757-899X/279/1/012037

Persistent-current magnetizations of Nb_3Sn Rutherford cables and extracted strands

E W Collings[1], M D Sumption[1], C S Myers[1], X Wang[2], D R Dietderich[2], K. Yagotyntsev[3] and A Nijhuis[3]

1. Center for Superconducting and Magnetic Materials (CSMM), Dept. of Materials Science and Engineering, The Ohio State University, Columbus, OH, USA. Corresponding author e-mail: sumption.3 @osu.edu
2. Superconducting Magnet Group, Lawrence Berkeley National Laboratory (LBNL), University of California, Berkeley, CA, USA
3. Energy, Materials, and Systems Group, the University of Twente, Enschede, NL

Abstract. The magnetizations of eight high-gradient quadrupole cables designated HQ and QXF and a pair of strands, identical in architecture but with different effective strand diameters extracted from an HQ and a related QXF cable, were measured. In the service of field quality assessment, the cable magnetizations and losses were measured by pickup coil magnetometry at 4.2 K in face-on fields, B_m, of ± 400 mT at frequencies, f, of up to 60 mHz. Based on the coupling component of loss, Q_{coup}, the coupling magnetization $M_{coup} = Q_{coup}/4B_m$ was derived for a ramp rate of 7.5 mT/s. Persistent current (shielding) magnetization and loss (M_{sh} and $Q_{h,strand}$) were measured on short pieces of extracted strand by vibrating sample magnetometry at 4.2 K. Unpenetrated *M-B* loops to ± 400 mT and fully penetrated loops to ± 14 T were obtained. M_{coup} can be easily controlled and reduced to relatively small values by introducing cores and adjusting the preparation conditions. But in low fields near injection Nb_3Sn's high J_c and correspondingly high $M_{sh,cable}$ may call for magnetic compensation to preserve field quality. The suitably adjusted cable and strand fully penetrated *M-B* loops were in reasonable accord leading to the conclusion that strand magnetization is a useful measure of cable magnetization, and that when suitably manipulated can provide input to magnet field error calculations.

1. Introduction

1.1 High Field Nb_3Sn Magnets

Rutherford cables wound with Nb_3Sn strands will be used in all the high field superconducting magnets required for ongoing and planned upgrades to the large hadron collider (LHC), viz. the high luminosity LHC (High Lumi LHC, HL-LHC, 11 and 12 T), a higher energy LHC (HE-LHC, 16 T), and a very high energy future circular collider (FCC, 16 T) [1]. Initiated in 2014 and planned for completion around 2024-26 is a set of high field magnets for the HL-LHC upgrade project [2][3] intended to produce 5-10-fold increases in the LHC's luminosity. Final beam focusing for the ATLAS and CMS detectors will be accomplished by four pairs of Nb_3Sn-wound quadrupoles with peak coil fields of 12 T [3]. Also as part of the upgrade, in order to make room for additional collimators in the dispersion-suppressor segments of the ring, some existing 8.33 T 15 m long NbTi dipoles will be replaced by 11 T 11 m long Nb_3Sn dipoles [4][5] [6][7].

Initially suggested in 2001, a higher energy successor to the LHC, the HE-LHC, would collide two proton beams circulating in the LHC tunnel [1][4][8][9][10][11]. A ring of about 1280 14 m long

16 T Nb_3Sn dipoles would support a center-of-mass collision energy of 27 TeV, close to the limit allowed by the tunnel's radius.

In addition to the HE-LHC is a proposed 100 TeV "future circular collider" (FCC). To be housed in a new tunnel 100 km in circumference the FCC is estimated to require 4578 15 m long 16 T Nb_3Sn dipoles [11][12][13]. Accordingly a 16 T Nb_3Sn dipole will be developed to satisfy the requirements of both the FCC and the HE-LHC. In contributing to that development, the US Magnet Development Program will be exploring the limits of applicability of Nb_3Sn for high field magnets [14]. For example in 2015 the Fermi National Accelerator Laboratory (FNAL) reported on the designs of four-layer cosine-theta Nb_3Sn dipoles with maximum bore fields (4.3 K) of 15.7 -16.3 T and a 15 T dipole demonstration magnet for a 100 TeV collider [15], and the Lawrence Berkeley National Laboratory (LBNL) designed a four-layer canted-cosine-theta 16 T Nb_3Sn dipole to satisfy the same need [13].

1.2 Nb_3Sn Strand and Cables for Accelerator Magnets

The numerous planned accelerator applications will demand a continuous supply of Nb_3Sn strand and cables capitalizing on the achievements of conductor development programs in the US (CDP) and Europe (NED) [1]. Studies of Nb_3Sn cable and strand properties are under way at FNAL [16]. Reported elsewhere are the effects of core type, placement, and width and heat treatment condition on interstrand coupling properties of Nb_3Sn cables[17][18]; important properties of strands are the field dependent critical current density, $J_c(B)$, and the effective filament diameter, d_{eff}. Magnetization due to ramp-rate-dependent interstrand coupling currents in cables and persistent currents in strands induce multipoles in the bore fields of dipole and quadrupole magnets [19][20]. Persistent-current magnetizations in Nb_3Sn strands, which being proportional to $J_c(B)d_{eff}$ are much stronger than in the LHCs NbTi, demands special attention. As a contribution to this topic, and indirectly to the US LHC Accelerator Research Program (LARP), we report on the magnetizations of: (i) LARP high gradient quadrupole cables designated HQ and QXF [18], (ii) a pair of strands, identical in architecture but with different d_{eff}s, that had been extracted from a LARP HQ and a related LARP QXF cable.

2. Experimental

2.1. Cable and Strand Samples

Several coils of the stainless-steel-cored HQ- and QXF-type Nb_3Sn Rutherford cables wound at LBNL were supplied for measurement to the Ohio State University's Center for Superconducting and Magnetic Materials (OSU-CSMM). Some cable and strand details are given in Tables 1 and 2, see also [18].

Table 1. Cable details

LBNL name	*	HQ1020 ZB	HQ1021 ZB	QXF 1055z-C	QXF 1055z-K	QXF 1055z-Q	QXF 1055z-O	QXF 1055z-M	QXF 1055z-D
OSU name	**H1**	**H2**		**Q1**	**Q2**	**Q3**	**Q4**	**Q5**	**Q6**
Strand count	35	35	35	40	40	40	40	40	40
pack factor, %	85.54	85.55	85.53	87.04	86.89	87.03	86.98	86.80	87.38
Core width, mm	0	8	--	11.9	15.9	15.4	14.3	13.3	0
Core cover, %	0	60	--	72	96	93	86	80	0

* Mixture of 1020 and 1021with cores extracted

Table 2. Strand details

Cable Type (Table II)	HQ	QXF
Strand source, type	OST-RRP,108/127	OST-RRP,108/127
Strand diam., d_s, mm	0.778	0.852
SC filament count	108	108
Filament OD, d_0, μm	51.5	62.2
Eff. fil. diam., d_{eff}, μm[(b)]	61.8	72.4

Cut pieces (50 cm long) of HQ and QXF cable were first enclosed in s-glass braid. The HQ cables were mounted five-high into bolt-down fixtures designed to apply side constraint as they were uniaxially compressed to 20 MPa at CSMM in preparation for heat treatment (HT) at Brookhaven National Laboratory. Four braid-coated lengths of QXF cable were sent to LBNL for mounting and HT in the same fixture but adjusted to confine the cable stack in a space just large enough to contain it during HT when expansions of 1.5% in width and 4.5% in thickness take place.

After HT the fixtures were returned to CSMM where the cable stacks were wrapped in teflon film, placed in an aluminum mold: (i) under uniaxial pressure of 5 MPa (the HQ stacks) or (ii) under negligible pressure (the QXF stacks) and vacuum impregnated with CTD-101 resin.

2.2 Cable and Strand Magnetization

2.2.1. Cable Measurement: Equipment located at the Energy, Materials, and Systems Laboratory of the University of Twente [21] was used to measure the calorimetric loss [18] and magnetization loss, $Q_t = \int M_t dB$ of the eight cable stacks at 4.2 K in transverse ("face-on", FO) AC fields of amplitude, B_m, = 400 mT at frequencies, f, of up to 60 mHz. In addition, cable stack Q4 was measured in B_m = 0.1- 1.4 T at 10 mHz; an experiment that yielded a set of nested *M-B* loops. In general, the total loss measured is $Q_t(f) = Q_h + Q_{coup}(f)$ where Q_h is the cable's/strand's hysteretic or persistent-current loss and $Q_{coup}(f)$ is the interstrand coupling loss (see below). Calorimetric loss was measured by the He-boil-off technique and calibrated against ohmic loss generated by a submerged 25 Ω resistor. For calibration of the installed pick-up coil magnetometer, the magnetization loss of cable stack H2 was equated to its calorimetric loss around the maximum of $Q_t(f)$. A second such calibration was applied to cable stack Q4's nested loops in terms of the B_m = ±1.4 T loop.

2.2.2. Strand Measurement: Short pieces of strand extracted from the ends of HT cable stacks were measured using the vibrating sample magnetometer attachment of a Quantum Design Model 6000 Physical Property Measurement System (PPMS). Unpenetrated *M-B* loops to ± 400 mT and fully penetrated loops to ± 14 T were obtained at 4.2 K.

3. Cable Loss and Magnetization

As explained in [18] the coupling loss per cycle per m^3 of cable (width, w, thickness, t, strand count, N, transposition pitch, $2L_p$) exposed to an FO field linearly ramping at a rate dB/dt is given by:

$$Q_{coup(FO)} = \left(\frac{4}{3}\right)\left(\frac{w}{t}\right)L_p B_m \left(\frac{N^2}{20}\right)\left[\frac{1}{R_c} + \frac{20}{N^3 R_a}\right].\left(\frac{dB}{dt}\right) \tag{1}$$

where R_c and R_a are the cable's crossover and adjacent interstrand contact resistances. Then after transforming dB/dt to a sinusoidal frequency, f, as explained in [22] we find:

$$Q_{coup(FO)}(f) = \left(\frac{\pi^2}{30}\right)\left(\frac{w}{t}\right)L_p B_m^2 N^2 \left[\frac{1}{R_c} + \frac{20}{N^3 R_a}\right].f \tag{2}$$

$$= \left(\frac{\pi^2}{30}\right)\left(\frac{w}{t}\right)L_p B_m^2 N^2 \left[\frac{1}{R_{eff}}\right].f \tag{3}$$

Figure 1 displays the total magnetization loss as function of frequency for the H series and QXF series cables. The lower set of curves represents the edge-on total loss measured calorimetrically ([18], Fig.1). The persistent current components, Q_h, are the f = 0 intercepts (FO and EO differ because of demagnetization effects [23]). The lack of a slope is due to the very low coupling currents in the EO orientation.

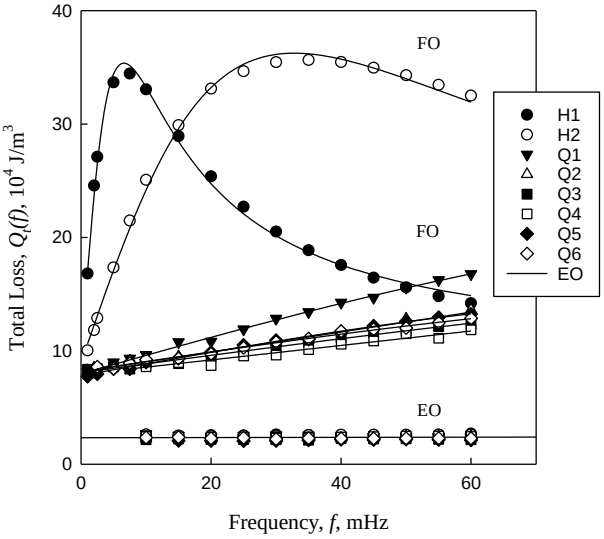

Figure 1. Total face-on (FO) magnetization loss, Q_t, as function of frequency, f, for the H series and QXF series cables. The lower set of curves represents the edge-on (EO) total loss measured calorimetrically ([18], Fig.1). The persistent current components, Q_h, are the $f = 0$ intercepts.

After substituting R_{eff} from the experimental dQ_t/df (equation (3), Figure 1, initial slopes) into equation (1) the coupling magnetization $M_{coup} = Q_{coup}/4B_m$ at a typical accelerator charging ramp rate of 7.5 mT/s can be calculated, Table 3.

Table 3. Coupling Magnetizations, $M_{coup} = Q_{coup}/4B_m$, at a ramp rate of 7.5 mT/s and unpenetrated persistent current loss at ± 400 mT

Cable Type	HQ		QXF					
Stack name	H1	H2	Q1	Q2	Q3	Q4	Q5	Q6
M_{coup}, kA/m	206.5	47.1	4.06	2.09	1.73	1.51	2.21	1.84
Q_h, 10^4J/m^3	9.19	8.97	7.95	8.14	8.12	7.92	7.92	8.30

Since the magnetic Q_t data were taken at B_m = ± 400 mT they embody only the unpenetrated Q_h components. It is interesting to note in passing that $<Q_h>_{HQ\text{-}set}/<Q_h>_{QXF\text{-}set}$ = 1.14 which is very close to the inverse ratios of the strand d_{eff} values (1.17) as expected for unpenetrated magnetizations.

4. Strand Loss and Magnetization

The 4.2 K measured unpenetrated *M-B* loops to ± 400 mT and fully penetrated loops to ± 14 T are presented in Figures 2 and 3, respectively. As indicated in Table 2 the strands extracted from HQ-cable H1 and QXF-cable Q6 were identical in design and differed only in diameter, d, and hence effective filament diameter, d_{eff}. We would expect the loop areas, Q_h, to respond to this such that for the fully penetrated loops $Q_{h,H1}/Q_{h,Q6} = d_{eff,H1}/d_{eff,Q6}$ while for the unpenetrated loops the inverse should hold.

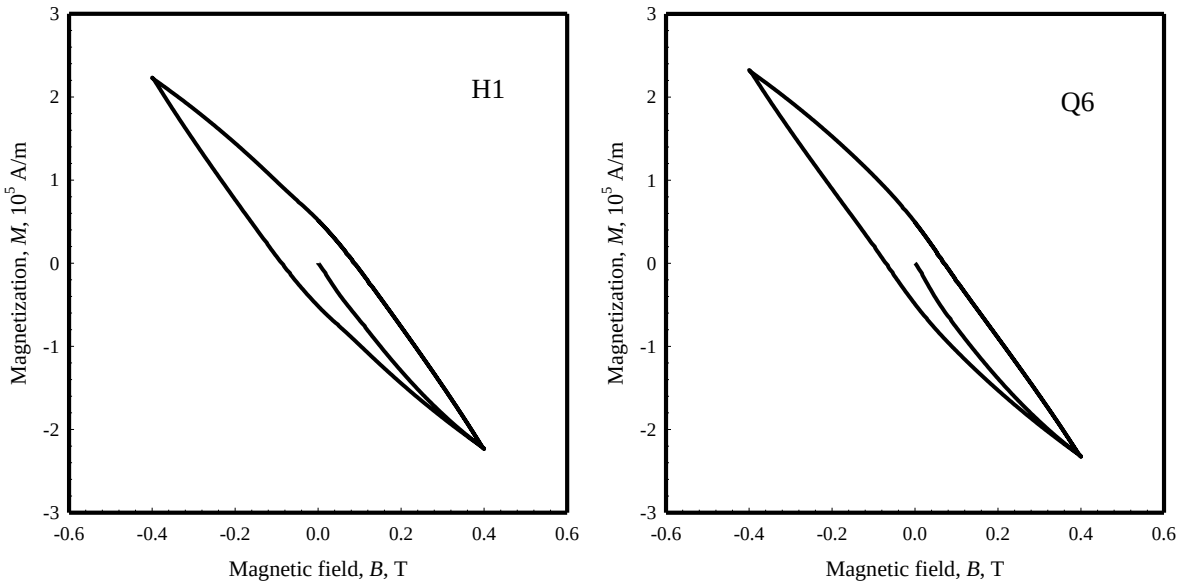

Figure 2. PPMS-measured unpenetrated *M-B* loops at 4.2 K to ± 400 mT

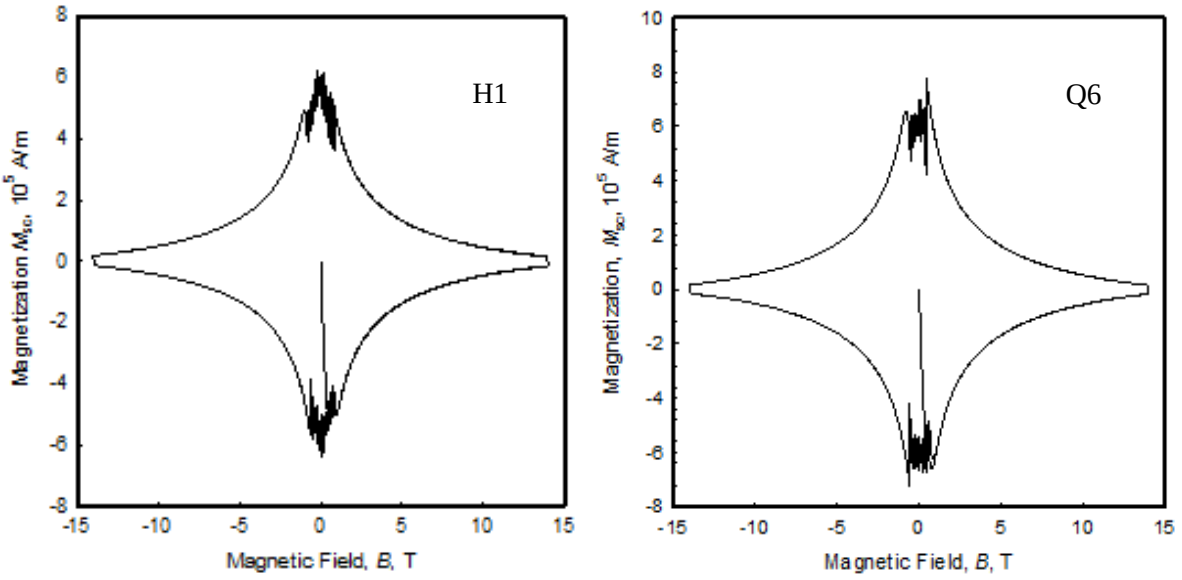

Figure 3. PPMS-measured penetrated *M-B* loops at 4.2 K to ± 14 T.

Both coupling magnetization and persistent current magnetization induce unwanted multipoles in dipole and quadrupole magnets [19][20]. The cable's coupling magnetization can be easily controlled and reduced to relatively small values by introducing cores and/or adjusting the preparation conditions (Table III, [18]). The cable's strand-based persistent current magnetization, which rises to very large values at low fields near injection calls for compensation e.g. by the use of magnetic shims [20]. In preparation for persistent current field error analysis the cable or strand is exposed to a suitable magnetization pre-cycle. In the present study we simply focus on the shielding branches of the *M-B* loops in Figure 3. To improve the relevance of the strand results to future Nb_3Sn accelerator cable applications we have: (i) introduced a cable fill factor of 87% , (ii) dropped the temperature from 4.2 K to 1.9 K and extrapolated the applied field to 16 T [24]. These estimated shielding magnetizations, $M_{sh,cable}$, of cables H1 and Q6 are presented and compared with the coupling results, in Figure 4.

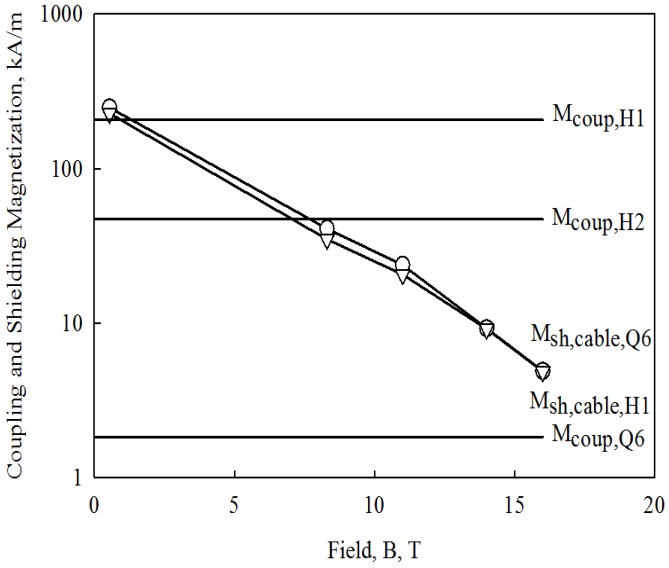

Figure 4. Coupling magnetizations 7.5 mT/s of cables H1, H2, and Q6 ($M_{coup,H1}$, $M_{coup,H2}$, and$M_{coup,Q6}$) and the estimated shielding magnetizations of cables H1 and Q6 ($M_{sh,cable,H1}$ and $M_{sh,cable,Q6}$) at 1.9 K based on strand magnetizations and a cable fill factor of 87%

5. Cable and Strand Magnetizations

5.1. Unpenetrated Persistent Current Strand/Cable Comparisons

Listed in Table 4 are the magnetically measured FO persistent current losses, Q_h, at B_m = ± 400 mT for all the cable stacks. We note that the averages for types HQ and QXF stacks are 9.078 and 8.057 x10^4J/m^3, respectively; a ratio of 1.14 compared to a d_{eff} inverse ratio (Table 1) of 1.17. Table 4 compares these magnetic FO Q_h values with the calorimetric EO values (Figure 1) and those derived from the *M-B* loops of Figures 2(a) and 2(b). The positioning of the strand Q_hs between the FO and EO cable values is a result of demagnetizations associated with the FO- and EO- oriented highly aspected Rutherford cables (see also [25] Table 4).

Table 4. Unpenetrated persistent current losses, Q_h, 10^4 J/m^3, of cables exposed to FO and EO applied fields and those of corresponding extracted strands

Cable Type	HQ		QXF					
Strand name	H1	H2	Q1	Q2	Q3	Q4	Q5	Q6
Q_h(FO)	9.19	8.97	7.95	8.14	8.12	7.92	7.92	8.30
Q_h(EO)	2.43	2.49	2.63	2.14	2.18	2.34	2.02	2.34
$Q_{h,,cable\text{-}strand}$*	4.38							4.09
$Q_{h,\,strand}$	5.03							4.70

* Based on $Q_{h,strand}$ adjusted for a cable packing factor of 87%

5.2 Penetrated Persistent Current Strand/Cable Comparisons

Figure 5 compares the fully penetrated *M-B* loop for cable stack Q4 (magnetically measured at 10 mHz to ±1.4 T) to that of a corresponding strand, in this case extracted from Cable Q6. Just as in the unpenetrated case strand magnetization is a useful measure of cable magnetization and as has been shown elsewhere [20] can provide input to magnet field error calculations.

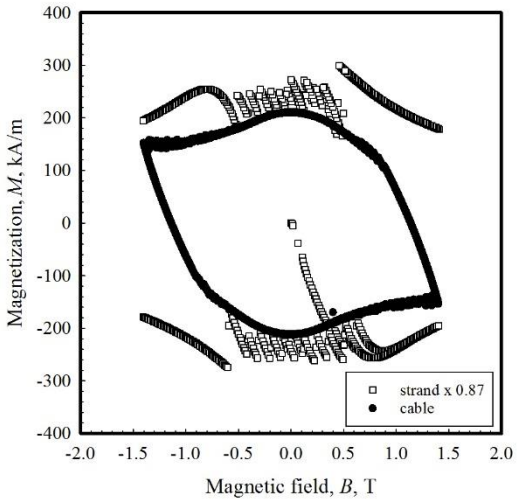

Figure 5. Comparison of penetrated "cable" *M-B* loops to ±1.4 T. For this purpose the strand loop height was modified by 0.87, a cable packing factor. The actual cable loop height measured at 10 mHz was reduced by 7.4% to remove the coupling component.

6. Summary

Magnetizations in the magnet windings induce multipoles in the bore fields of dipole and quadrupole magnets. Strand and cable magnetization data can provide a useful input to field error calculations. As a contribution to this topic, and indirectly to the US LHC Accelerator Research Program (LARP), we have measured the magnetizations of: (i) eight LARP high gradient quadrupole cables designated HQ and QXF, (ii) a pair of strands, identical in architecture but with different d_{eff}s, that had been extracted from a LARP HQ and a related LARP QXF cable.

The magnetization losses, of the eight cable stacks were measured by pickup coil magnetometry at 4.2 K in FO fields, B_m, of ± 400 mT at frequencies, f, of up to 60 mHz. The total loss is $Q_t(f) = Q_h + Q_{coup}(f)$ where Q_h is the cable's/strand's hysteretic or persistent-current loss and $Q_{coup}(f)$ is the interstrand coupling loss. Based on Q_{coup} the coupling magnetization $M_{coup} = Q_{coup}/4B_m$ was derived for a ramp rate of 7.5 mT/s. Persistent current (shielding) magnetization and loss (M_{sh} and $Q_{h,strand}$) were also measured on short pieces of strand extracted from the ends of heat treated cable stacks by vibrating sample magnetometry at 4.2 K. Unpenetrated *M-B* loops to ± 400 mT and fully penetrated loops to ± 14 T were obtained. Thus the cables' M_{coup}s were directly measured and their $M_{sh,cable}$s indirectly measured in terms of the strands' shielding magnetizations, M_{sh}, modified by a cable packing factor of 87%.

M_{coup}, which has no field-dependent components, can be easily controlled and reduced to relatively small values by introducing cores ($M_{coup,H2,cored}/M_{coup,H1,uncored}$ = 0.23) and adjusting the preparation conditions $M_{coup,Q6,prep}/M_{coup,H1,uncored}$ = 0.009). $M_{sh,cable}$ is proportional to $J_c d_{eff}$ in response to which: (1) The ratio $M_{sh,H1}/M_{sh,Q6}$ turned out to be equal to the ratio of the strands' d_{eff}s. (2) In low fields near injection Nb_3Sn's high J_c leads to a correspondingly high $M_{sh,cable}$ Thus at 0.54 T $M_{sh,cable,Q6}$ is over 100 times greater than $M_{coup,Q6}$ which calls for the introduction of some form of magnetic compensation to preserve field quality.

In terms of unpenetrated persistent current loss the directly measured cable Q_h was in reasonable accord with the strand derived $Q_{h,cable\text{-}strand}$. Likewise the suitably adjusted cable and strand fully penetrated *M-B* loops were in reasonable accord. These observations led to the conclusion that strand magnetization is a useful measure of cable magnetization, and that when suitably manipulated can provide input to magnet field error calculations.

Acknowledgments

Funding was provided by the U.S. Department of Energy, Office of High Energy Physics, under Grants No. DE-SC0010312 and DE-SC0011721 (OSU) and DE-AC02-05CH11231 (LBNL). The cables were wound by H.C. Higley (LBNL), heat treated at LBNL (QXF cables) and Brookhaven National Laboratory (A.K, Ghosh, HQ cables). J. Yue and R. Avonce (HyperTech Research) performed the vacuum impregnation.

References

[1] Bottura, L de Rijk G Rossi L and Todesco E 2012 *IEEE Trans. Appl. Supercond.* **22** 4002008
[2] Barachetti A Szeberenyi A and Rossi L 2016 Final Project Report, HiLumi LHC, *CERN-ACC-2016-0007*, 12 January.
[3] Ambrosio G 2015 *IEEE Trans. Appl. Supercond.* **25** 4002107.
[4] Apollinari G 2014 5th International Particle Accelerator Conference (IPAC 2014) 16-20 Jun, Dresden, Germany (4 pp); FERMILAB-CONF-14-326-TD
[5] Apollinari G 2017 HL-LHC and HE-LHC APS April Meeting, January 28–31, Washington, DC
[6] Karppinen M Andreev N Apollinari G 2012 *IEEE Trans. Appl. Supercond.* **22** 4901504.
[7] Karppinen M 2012 11 T Dipole Status May 2012, https://espace.cern.ch/dsdipole/-; see also: hilumilhc.web.cern.ch/hilumilhc/activities/11-T/WP11/
[8] Assmann R Bailey R Brüning O Dominguez O de Rijk G Jimenez JM Myers S Rossi L Tavian L Todesco E and Zimmermann F 2010 *CERN-ATS-2010-177*.
[9] Brüning O Dominguez O Myers S Rossi L Todesco E Zimmermann F 2011 *EuCARD-AccNet-EuroLumi Workshop: The High-Energy Large Hadron Collider*, Malta, 14-16 Oct 2010; CERN Yellow Report CERN-2011-003, pp. 7-14
[10] Zimmermann F 2016 *Challenges and Goals for Accelerators in the XXI Century*, World Scientific, pp. 513-522.
[11] Benedikt M and Zimmermann F 2017 3rd Annual Meeting of the Future Collider Study, Intercontinental Hotel, Berlin, Germany, May 29-June 2.
[12] van Nutgeren J Schoerling D Kirby G Murtomaki J de Rijk G Rossi L Bottura L ten Kate H H J and Dhallé M 2016 *IEEE Trans Appl. Supercond.* **26** 4003206.
[13] Caspi S Arbelaez D Brouwer L Gourlay S Prestemon S and Auchmann B 2017 *IEEE Trans Appl. Supercond.* **27** 4001505.
[14] Goulay S A Prestemon S O Zlobin A V Cooley L and Larbalestier D 2016 The US Magnet Development Program Plan, *Lawrence Berkeley National Laboratory Report No.* LBNL-1006046.
[15] Zlobin A V Andreev N Barzi E Kashikhin V V and Novotski I 2017 *Proc. IPAC 2015*, Richmond, VA 3365-3367 ; also Zlobin A 2017 *US-MDP First General Meeting and Workshop*, Marriott Napa Valley, Feb. 6-8.
[16] Barzi E Li P Turrioni D Xu X and Zlobin A 2017 presentation at the 25TH Magnet Technology Conference, MT25, August 27-31, Amsterdam, NL
[17] Collings E W Sumption M D Majoros M Wang X, et al., 2015 *IEEE Trans. Appl. Supercond.* **25** 4802805.
[18] Collings E W Sumption M D Majoros M Wang X Dietderich D R Yagotyntsev K and Nijhuis A 2017 *IEEE Trans. Appl. Supercond.* **27** 0601305.
[19] Wang X Ambrosio G Borgnolutti F Buehler M Chlachidze G Dietserich D R DiMarco J Felice H Ferracin P Ghosh A Godeke A Marchevsky M Orris D Prestemon S O Sabbi G Sylvester C Tartaglia M Todesco E Velev G and Wanderer P 2014 *IEEE Trans. Appl. Supercond.* **24** 4002607.
[20] Wang X Ambrosio G Chlachidze G DiMarco J Ghosh A K Holik E F Prestemon S O Sabbi G L and Stoynev S E 2017 *IEEE Trans. Appl. Supercond.* **27** 4000805.
[21] Verweij A P 1995 Electrodynamics of Superconducting Cables in Accelerator Magnets *Ph.D. Thesis*, University of Twente Press, p. 94.
[22] Sumption M D Collings E W Scanlan R M Nijhuis A and ten Kate H H J 1999 *Cryogenics* **39** 1-12.
[23] Collings E W Sumption M D Susner M A Dietderich D Kroopshoop E and Nijhuis A, IEEE Trans. Appl. Supercond. 2013 **23** 4702305
[24] Summers L T Guinan M W Miller J R and Hahn P A 1991 *IEEE Trans. Magnetics* **27** 2041-2044.
[25] Collings E W Sumption M D Susner M A Dietderich D R Kroopshoop E and Nijhuis A 2012 *IEEE Trans. Appl. Supercond.* **22** 6000904.